

A Compact Design of Planar Array Antenna with Fractal Elements for Future Generation Applications

Naser Ojaroudiparchin, Ming Shen, and Gert Frølund Pedersen

Antennas, Propagation, and Radio Networking (APNet) Section
Department of Electronic Systems, Faculty of Engineering and Science
Aalborg University, DK-9220, Aalborg, Denmark
naser@es.aau.dk, mish@es.aau.dk, gfp@es.aau.dk

Abstract — In this paper, a planar phased array fractal antenna for the future fifth generation (5G) applications is presented. The proposed array antenna is designed to operate at 22 GHz. 64 patch antenna elements with coaxial-probe feeds have been used for the proposed design. The antenna elements are based on Vicsek fractal geometry where the third iteration patches operate over a wide bandwidth and contribute to improve the efficiency and realized gain performance. The designed planar array has more than 22 dB realized gain and -0.3 dB total efficiency when its beam is tilted to 0° elevation. The antenna configuration is simple, easy to fabricate and can be integrated into 5G devices. Simulated and measured results are presented to validate the usefulness of the proposed phased array antenna for 5G applications.

Index Terms — 5G wireless communications, fractal antenna, patch antenna, planar phased array.

I. INTRODUCTION

Due to the increasing need for future applications requiring even higher data rates (such as wireless broadband connections, massive machine type communications and highly reliable networks), the research and development of fifth-generation (5G) mobile communication systems have started. It is predicted that the commercial deployment of 5G will be approximately in the early of 2020s [1-3]. One major difference in the enabling technologies for 4G and 5G communication is the use of millimeter wave (mm-Wave) frequencies, aiming for wider bandwidth and higher spectral efficiency [4]. However, moving from the cellular carrier frequencies used today (<4 GHz) up towards the mm-Wave bands introduces new aspects that need careful consideration [5-7].

As a solution to minimizing the antenna size while keeping high radiation efficiency, fractal antennas have drawn special attention in microwave engineering. In many cases, the use of fractal element antennas can simplify circuit design. Another benefit of fractal

antennas is that, fractal antennas are in form of a printed circuit board (PCB), which can reduce fabrication costs.

Basically, a fractal is a rough or fragmented geometric shape that can be subdivided in parts, each of which is a reduced-size copy of the whole. Fractals are generally self-similar and independent of scale. Fractal antenna theory uses a modern (fractal) geometry that is a natural extension of Euclidian geometry [8-10].

This paper focuses on the design and implementation of a planar phased array fractal antenna for millimeter-wave 5G mobile applications. The proposed design shown in Fig. 1 consists of 64-elements of 22 GHz Vicsek fractal patch antenna elements with coaxial-probe feed. The proposed phased array antenna has high efficiencies, high gains and good beam steering characteristics. The analysis and performance of the antenna are obtained by using CST software [11].

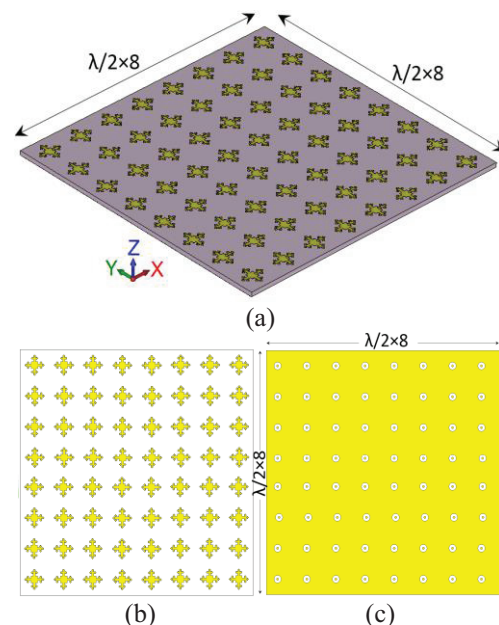


Fig. 1. Proposed antenna configuration: (a) side view, (b) top layer, and (c) bottom layer.

II. ANTENNA DESIGN

The fractal geometries are generated by an iterative process performed on a simple starting topology. As can be observed in Fig. 2 (a), the proposed fractal shape begins as a simple square (0th order). Next, divide the square into nine equal small squares and move the four at comers [9].

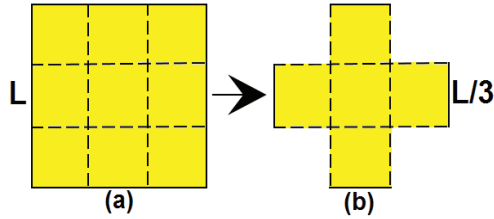


Fig. 2. Generating rules of Vicsek shape: (a) the 0th order and (b) the 1st order.

According to the properties of self-similarity, the fractal dimension D_s is defined as:

$$D_s = \frac{\log(N)}{\log(R)}, \quad (1)$$

where N is the total number of distinct copies similar to (1), which is scaled down by a ratio of $1/r$. For the Vicsek shape, $N=5$ and $r=3$. So the fractal dimension is:

$$D_s = \frac{\log 5}{\log 3} = 1.4650.$$

The resonant frequencies can be carried out using the following equation [12]:

$$(f_r)_{mn} = \frac{1}{2\pi \sqrt{\left(\frac{m\pi}{l}\right)^2 + \left(\frac{n\pi}{w}\right)^2}} \Big|_{l=w} = \frac{c}{2l\sqrt{\epsilon_r}} \sqrt{m^2 + n^2}, \quad (2)$$

where (f_r) is the mn mode resonant frequency, l , w are the two dimensions ($w=l$) of the square, and c is the velocity of light. The fundamental frequency corresponds to 22 GHz by using the equation above.

As illustrated in Fig. 1, 64-elements of Vicsek fractal patch antenna have been used for the proposed design. For beam forming array, the distance between antenna elements (d) is calculated near $\lambda/2$ ($f_0=22$ GHz). The overall dimension of the proposed planar phased array antenna is $8\lambda/2 \times 8\lambda/2$.

III. SINGLE ELEMENT FRACTAL PATCH ANTENNA

In this section the fundamental properties of the designed Vicsek fractal patch antenna have been investigated. The geometry of the single element patch antenna is illustrated in Fig. 2. A microstrip patch antenna is basically a conductor printed on the top layer of the substrate with a full ground plane. It can be fed in a variety of ways such as microstrip feed, coaxial feed, aperture coupled feed, and proximity coupled feed [13].

In this paper, the coaxial probe feeding technique has been used. The basic geometry of the radiation patch is a square of length L , on which repeated iterations lead to the Vicsek snowflake geometry as shown in Fig. 3.

As illustrated, the fractal shape begins as a simple square which its iteration order is zero [Fig. 4 (a)]. Next, divide the square into nine equal small squares and move the four at comers [Fig. 4 (b)]. In order to obtain the second and third iteration [Figs. 4 (c) and (d)], the same process is applied for the small squares located at the corners of radiation patch. The values of the antenna parameters are listed in Table 1.

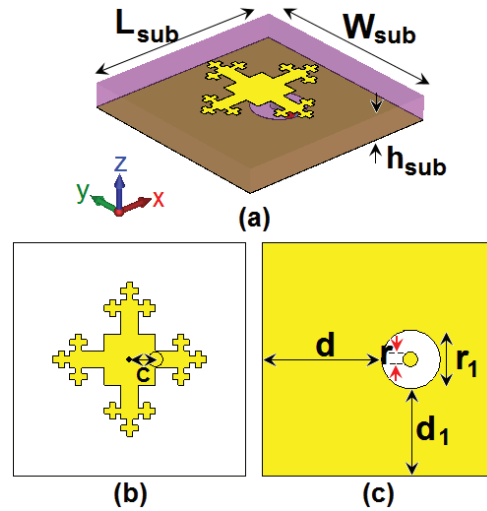


Fig. 3. Configuration of single element antenna: (a) side view, (b) top layer, and (c) bottom layer.

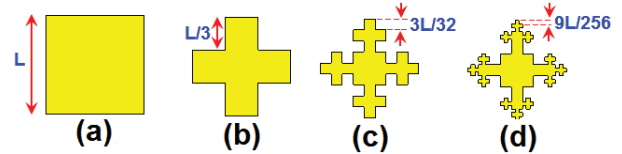


Fig. 4. Vicsek snowflake in its different iteration stages: (a) basic geometry, (b) first iteration, (c) second iteration, and (d) third iteration.

Table 1: Dimensions of the antenna parameters

Parameter	W_{sub}	L_{sub}	h_{sub}	L
Value (mm)	6.8	6.8	0.8	4.5
Parameter	r_1	d	d_1	C
Value (mm)	0.5	3.4	2.75	0.75

Figure 5 illustrates the simulated S_{11} characteristics of the patch antenna for iteration stages of the fractal geometry. It is observed that the Vicsek fractal geometry improves the impedance matching characteristic of the antenna at 22 GHz along the bandwidth enhancement of the antenna [14].

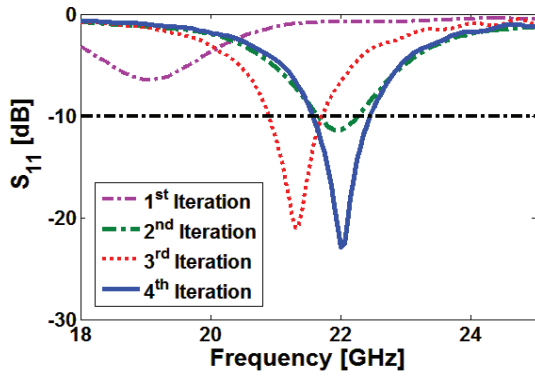


Fig. 5. Simulated S_{11} characteristics of the Vicsek fractal patch antenna for different iterations stages.

Figure 6 shows the simulated radiation patterns of the antennas shown in Fig. 4 at resonance frequencies. As illustrated, by using the proposed fractal structure, the efficiency and realized gain characteristics can be improved. It can be seen, the single element 22 GHz Vicsek patch has values of -0.1 dB and 6.8 dB for radiation efficiency and realized gain characteristics respectively.

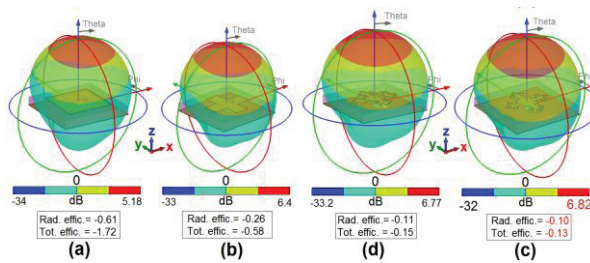


Fig. 6. Simulated radiation patterns at resonance frequencies of the antennas for different iteration stages shown in Fig. 4.

Figure 7 shows the simulated surface current distribution for the antenna at 22 GHz. As illustrated, the currents flow around the Vicsek fractal radiator. It can be seen, the distribution of the current around the radiation patch is almost uniform due to symmetrical configuration of the radiator. One of the important parameters of the proposed design is the feeding point. Its main effect occurs on the operation frequency of the antenna.

Figure 8 illustrates the simulated S_{11} characteristics with various values of C (distance between feeding point and center of the radiator). As the distance between feeding point and center of antenna increases from 0.6 to 0.8 mm, the operation frequency of antenna is varied from 21.6 to 22.2 GHz. From this result, we can conclude that the antenna operation frequency can be controlled by changing the antenna feeding point. For $C=0.75$ mm, the antenna has a good impedance

matching at the desired frequency (22 GHz).

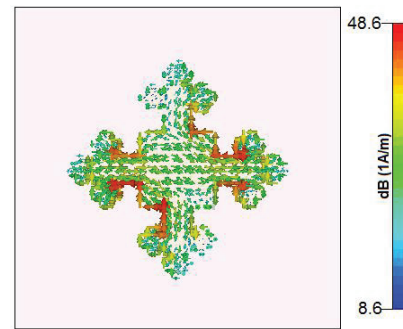


Fig. 7. Simulated surface current distribution of the single antenna element at 22 GHz.

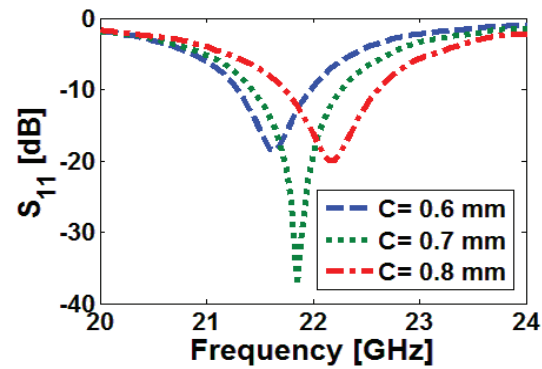


Fig. 8. Simulated S_{11} characteristics of the antenna for different values of C .

Simulated maximum gain, radiation and total efficiencies of the single element patch antenna over operation frequency range are illustrated in Fig. 9. As seen, the antenna radiation and total efficiencies are better than -0.2 and -1 dB, respectively. In addition, the antenna has more than 6.7 dBi maximum gain.

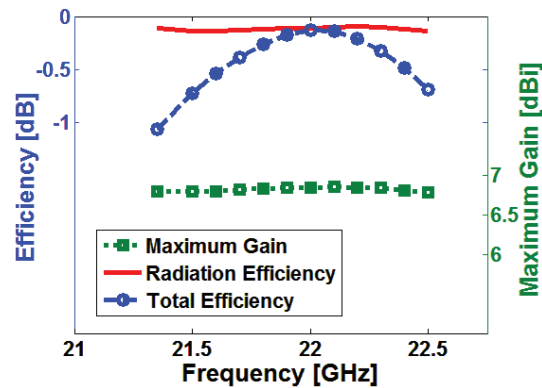


Fig. 9. Simulated maximum gain, radiation and total efficiencies of the antenna over the operation frequency range.

IV. 1×8 LINEAR ARRAY USING THE PROPOSED FRACTAL STRUCTURE

Figure 10 shows the configuration of the 1×8 linear array with eight elements of 22 GHz patch antennas. For beam forming array, the distance between elements is calculated $\lambda/2=6.8$ mm. The simulated S-parameters of the linear array are illustrated in Fig. 11.

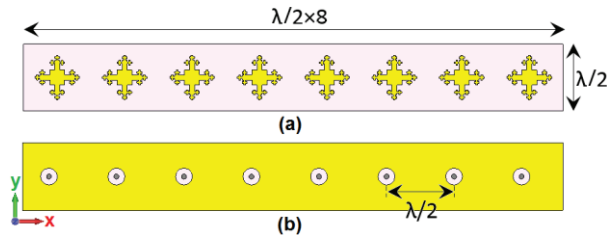


Fig. 10. Geometry of the linear array: (a) top layer and (b) bottom layer.

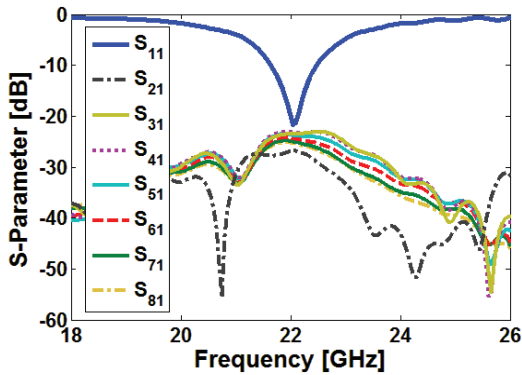


Fig. 11. Simulated S-parameters of the linear array.

As illustrated, the antenna can operate at the frequency range of 21.6 to 22.4 GHz. It can be seen that the antenna has -22 dB return loss and the highest mutual-coupling between the elements is less than -23 dB which is sufficient for beam steering issue.

3D beam steering characteristic of the array radiation patterns with realized gain values at different scanning angles (0°, 30°, and 60°) at 22 GHz are shown in Fig. 12. The analysis and performance of the antenna beams are obtained by post-processing using CST software. The shape and direction of the array beams are determined by relative phases amplitudes applied to each radiating element as below:

$$\psi = 2\pi(d/\lambda) \sin \theta, \quad (3)$$

where d is the distance between the radiation elements and θ is the angle of incidence. In order to see the radiation beam of the array at 30° (by considering that the elements are arranged on a linear array with distance of $\lambda/2$), the phase shift between adjacent sources will be calculated $\Psi=90^\circ$. The next step is applying 90° phased-shifting with same values of the

amplitude=1 for the radiation elements, respectively. Same process of the phase shifting could be used of the planar phased arrays.

As seen, the proposed antenna has a good beam steering property which is highly effective to cover the spherical beam-coverage for 5G devices. The beam-steering characteristic of the proposed antenna for plus/minus (+/-) scanning angles are expected to be the same.

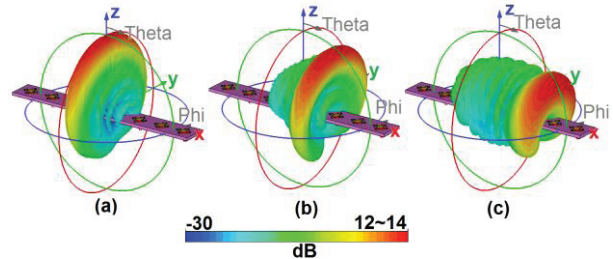


Fig. 12. 3D Radiation patterns of the linear array at different scanning angles: (a) 0°, (b) 30°, and (c) 60°.

Figure 13 illustrates the simulated directivity, radiation efficiency and total efficiency characteristics of the proposed antenna in the scanning range of 0 to 70 degree. As seen, the antenna radiation and total efficiencies are better than -0.5 dB (90%). Furthermore, as can be seen, when the scanning angle of beam-steering characteristic is $\leq +60$, the proposed antenna has more than 12 dBi directivity.

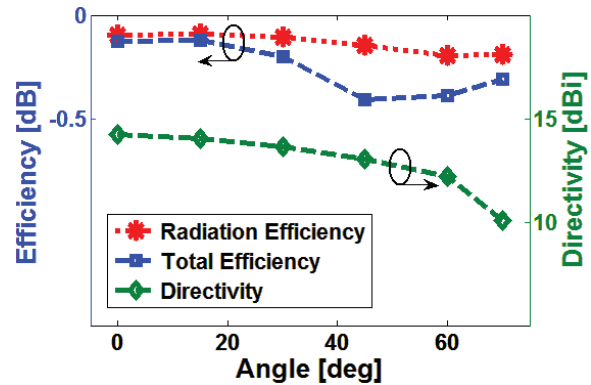


Fig. 13. Simulated directivity, radiation efficiency and total efficiency characteristics of the antenna at different scanning angles.

V. THE PROPOSED PLANAR PHASED ARRAY 5G ANTENNA

64 Vicsek patches have been used to design the final planar 5G antenna. The proposed planar array with final design has been fabricated to validate the performance. Figure 14 shows the photograph of fabricated antenna. The simulated and measured S_{11}

characteristics of the antenna element are shown in Fig. 15. As illustrated, the antenna has a good response in the frequency range of 21.5 to 22.5 GHz.

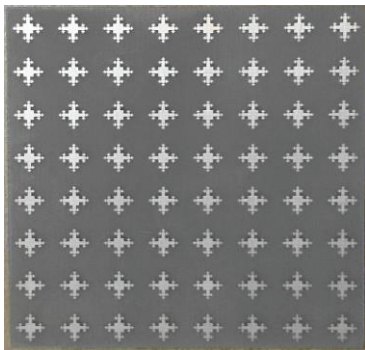


Fig. 14. Fabricated prototype (top-view).

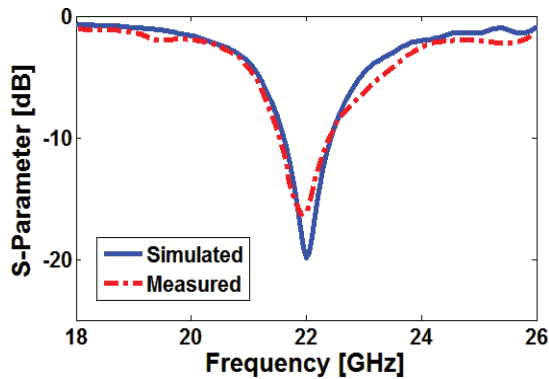


Fig. 15. Measured and simulated S_{11} characteristics of the proposed antenna.

Simulated surface-current distribution for the antenna at 22 GHz (resonance frequency) is shown at Fig. 16. As illustrated, the current flows are distributed around the fractal patch elements and the effect of the full ground plane to reduce the power of radiation is insignificant.

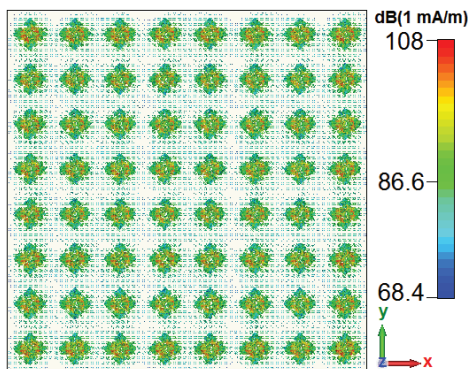


Fig. 16. Simulated current distribution of the proposed planar phased array at 22 GHz (resonance frequency).

Figure 17 shows the radiation beams of the proposed 8×8 phased array antenna with realized gain values for different scanning angles at 22 GHz. It can be seen, the antenna has a good beam steering characteristic with high-level gains at different scanning angles. In addition the proposed array has high efficiencies at different scanning angles.

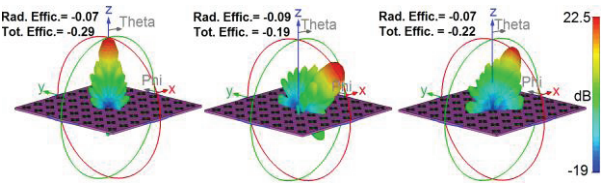


Fig. 17. 3D radiation patterns of the proposed planar array at different scanning angles.

Figure 18 shows the directivity characteristics of the single element, linear, and planar arrays of the proposed fractal patch antenna. It can be seen that the designed arrays have good performances. More than 7, 13, and 23 dBi directivity values with good radiation behaviors and low back lobes have been achieved for the arrays.

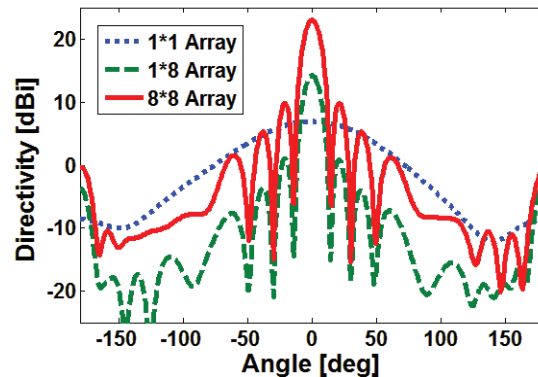


Fig. 18. Simulated directivity characteristics of the single element, linear, and planar array antennas at 0° scanning angle.

As can be observed in Fig. 1, eight 1×8 uniform linear arrays are used where each radiating element of them is excited by signals with equal magnitude. One of the most important system blocks to achieve a functional array antenna is the feed network. There are various feed network techniques that could be used for this purpose (such as the corporate feed network shown in Fig. 19). The power dividers (such as Wilkinson) divide the power to equally 1:N and also unequally by changing the input and output. The feed network of proposed phased array can be implemented using low loss phase shifters (such as HMC933LP4E) for beam steering issue. The HMC933LP4E phase shifter [15] is

controlled via an analog-control voltage from 0 to +13V. It has a low insertion loss characteristic in the operation frequency of 18-24 GHz.

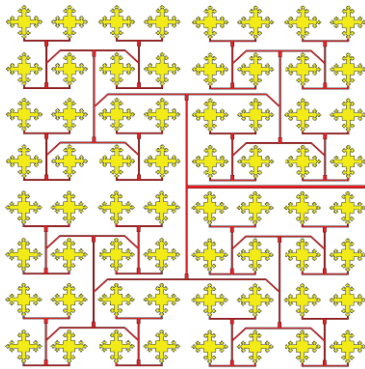


Fig. 19. Schematic of the corporate feed network for the planar phased arrays.

Compared with previous works [16-20], the proposed phased array antenna provides attractive features such as high-gain/high-directivity, low-profile/symmetric structure, high efficiency and easy to fabricate. Vicsek fractal radiation elements have been used as a solution to minimizing the antenna overall size while keeping high radiation efficiency. The overall dimension of the proposed design is $55 \times 55 \text{ mm}^2$. Using the fractal elements instead of conventional structure, the antenna provides superior antenna fundamental radiation performance. The values of the antenna gain, directivity and efficiency characteristics when its beam is tilted to 0° are 22.5 dB, 23 dBi, and -0.29 (93%).

The design and its radiation elements have symmetrical configurations which causes the antenna provides directional and symmetrical radiation patterns. Furthermore, the antenna has good beam-steering property with high-gain values and low side/back lobes at different angles. It also has wide-angle scanning which makes it suitable for phased array applications.

VI. INVESTIGATION ON THE ARRAY PERFORMANCE WITH DIFFERENT NUMBER OF RADIATORS

In this section, the investigation on the performance of the proposed 22 GHz planar array with different number of the patch antennas has been done.

Figure 20 shows the configurations of the arrays with 2×2 , 4×4 , and 8×8 numbers of antenna elements. The spacing between the elements of the arrays is $\lambda/2$ of 22 GHz. Figure 21 shows the simulated S-parameters (S_{11} & S_{21}) of the arrays. It can be seen that the designed arrays have good and similar performances.

As illustrated in Fig. 21 (a), -25, -28, and -35 dB reflection coefficients (S_{11}) are achieved for the 2×2 ,

4×4 , and 8×8 planar arrays. Figure 22 (b) shows the highest mutual couplings (S_{21}) between antenna elements for the proposed arrays. As can be observed, the designed arrays have sufficient mutual couplings between the radiation elements (less than -24 dB).

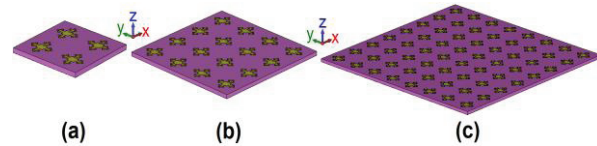


Fig. 20. Configuration of the planar arrays: (a) 2×2 , (b) 4×4 , and (c) 8×8 .

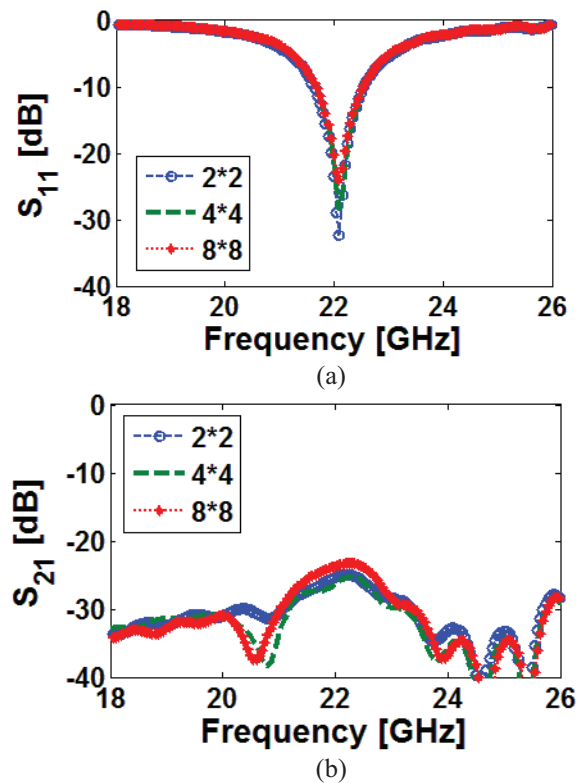


Fig. 21. (a) S_{11} and (b) S_{21} of the planar arrays.

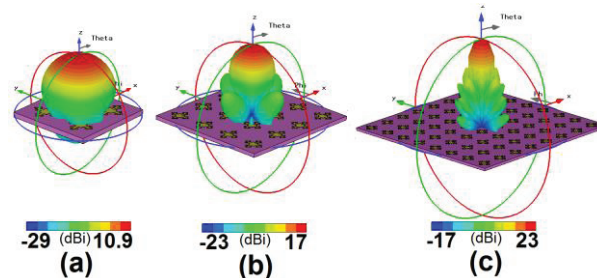


Fig. 22. 3D radiation beams of the planar arrays at 0° scanning angle for: (a) 2×2 , (b) 4×4 , and (c) 8×8 .

3D directional radiation beams of the arrays when their beams are tilted to 0° elevation are shown in Fig. 22. More than 10.9, 16.5, and 23 dBi directivity values with good radiation behaviors and low back/side lobes have been achieved for the planar arrays.

Table 2 summarizes the performances of the designed arrays in terms of realized gain, efficiency, bandwidth (BW), reflection coefficient (RC) and mutual coupling (MC). As seen, the arrays exhibit good performance in different terms of the antenna parameters.

Table 2: Characteristics of the planar arrays at 0°

Param.	Gain	Effic.	BW	RC	MC
1×1	6.82 dB	-0.13 dB	1 GHz	-23 dB	N/A
2×2	10.7 dB	-0.23 dB	0.9 GHz	-35 dB	-26 dB
4×4	16.7 dB	-0.28 dB	0.9 GHz	-28 dB	-26 dB
8×8	22.7 dB	-0.29 dB	0.9 GHz	-25 dB	-24 dB

VII. CONCLUSION

An 8×8 phased array 5G antenna with fractal patch elements is designed and investigated in this study. The antenna elements are designed based on Vicsek fractal geometry to operate at 22 GHz. The proposed antenna has good performance in terms of impedance matching, antenna gain, efficiency, and beam steering characteristics. The antenna also features compact and symmetric structure. The results show that the proposed antenna could be used in high speed wireless communication systems in particular for use in 5G mobile devices. In addition, the radiation characteristics of the proposed planar phased array with different number of the radiators have been investigated.

REFERENCES

- [1] P. Zhouyue and F. Khan, "An introduction to millimeter-wave mobile broadband systems," *IEEE Communications Magazine*, vol. 49, pp. 101-107, 2011.
- [2] T. S. Rappaport, et al., "Millimeter wave mobile communications for 5G cellular: It will work!," *IEEE Access*, vol. 1, pp. 335-349, 2013.
- [3] W. Roh, et al., "Millimeter-wave beamforming as an enabling technology for 5G cellular communications: Theoretical feasibility and prototype results," *IEEE Commun. Mag.*, vol. 52, pp. 106-113, 2014.
- [4] Y. Wang, et al., "5G mobile: Spectrum broadening to higher-frequency bands to support high data rates," *IEEE Vehicular Technology Magazine*, vol. 9, pp. 39-46, 2014.
- [5] S. Rajagopal, et al., "Antenna array design for multi-Gbps mm-wave mobile broadband communication," in *IEEE Globecom*, Dec. 2011.
- [6] T. S. Rappaport, et al., "Broadband millimeter-wave propagation measurements and models using adaptive-beam antennas for outdoor urban cellular communications," *IEEE Transactions on Antennas and Prop.*, vol. 61, no. 4, pp. 1850-1859, 2013.
- [7] T. Bai and R. Heath, "Coverage and rate analysis for millimeter wave cellular networks," *IEEE Transactions on Wireless Communications*, vol. 14, pp. 110-1114, 2015.
- [8] D. H. Werner and S. Ganguly, "An overview of fractal antenna engineering research," *IEEE Antennas and Propagation Magazine*, vol. 45, pp. 38-57, 2003.
- [9] W. Hongjian and G. Benqing, "The full wave analysis of fractal antenna," *3rd International Symposium on Electromagnetic Compatibility*, pp. 135-138, 2002.
- [10] B. B. Mandelbort, *The Fractal Geometry of Nature*. New York, W. H. Freeman, 1983.
- [11] CST Microwave Studio, ver. 2014, CST, Framingham, MA, USA, 2014.
- [12] C. A. Balanis, *Antenna Theory: Analysis and Design*. Wiley, New York, 1982.
- [13] R. Garg, P. Bhartia, I. Bahl, and A. Ittipiboon, *Microstrip Antenna Design Handbook*. Norwood, MA: Artech House, 2000.
- [14] C. Puente, J. Ponmeu, R. Pous, and A. Cardama, "On the behavior of the Sierpinski multiband antenna," *IEEE Transactions on Antennas and Propagation*, vol. 46, pp. 517-524, 1998.
- [15] HMC933LP4E, "Analog phase shifter," Hittite Microwave Company.
- [16] S. E. Valavan, D. Tran, A. G. Yarovoy, and A. G. Roederer, "Dual-band wide-angle scanning planar phased array in X/Ku-bands," *IEEE Trans. Antennas and Propagation*, vol. 62, pp. 2514-2521, 2014.
- [17] J. Wu, Y. J. Cheng, and Y. Fan, "Millimeter-wave wideband high-efficiency circularly polarized planar array antenna," *IEEE Trans. Antennas and Propagation*, vol. 64, pp. 535-542, 2014.
- [18] D. L. Lavanya, "Design of 8×8 circularly polarized planar array antenna for ISM band," *2012 International Conference on Radar, Communication and Computing (ICRCC)*, SKP Engineering College, Tiruvannamalai, TN, India, pp. 112-116, 21-22 Dec. 2012.
- [19] P. Padilla de la Torre and M. Sierra Castafiort, "Transmitarray for Ku band," *The Second European Conference on Antennas and Propagation (EuCAP)*, Edinburgh, UK, 11-16 Nov. 2007.
- [20] S. E. Valavan, D. Tran, A. G. Yarovoy, and A. G. Roederer, "Planar dual-band wide-scan phased array in X-band," *IEEE Trans. Antennas and Propagation*, vol. 62, pp. 5370-5375, 2014.



Naser Ojaroudiparchin was born in 1986 in Iran. He received M.Sc. degree in Telecommunication Engineering from Shahid Rajaei University (SRITU), Tehran, Iran in 2013. Since Nov. 2014, he is working as a Guest Researcher in Antennas, Propagation and Radio Networking (APNet) section, Department of Electronic Systems, Aalborg University, Aalborg, Denmark. His research interests include multi-band/UWB antennas, mm-Wave phased array 5G antennas, band-stop/band-pass microwave filters, and reconfigurable structure.



Ming Shen received the Master and Ph.D. degrees in Electrical Engineering from the University of Chinese Academy of Sciences, China in 2005, and from Aalborg University, Denmark in 2010, respectively. Since 2007, he has been with the Department of Electronic Systems, Aalborg University, where he is currently an Assistant Professor. He is the author of more than 30 technical papers and book chapters. His current research interests include: energy harvesting and battery-less low power circuits and systems, 5G mm-Wave circuits and antennas, remote patient monitoring, and wireless power transfer technologies.



Gert Frølund Pedersen received the B.Sc. E.E. degree, with honor, in Electrical Engineering from College of Technology in Dublin, Ireland in 1991, and the M.Sc. E.E. degree and Ph.D. from Aalborg University in 1993 and 2003. He has been with Aalborg University since 1993 where he is a Full Professor heading the Antenna, Propagation and Networking LAB with 36

researchers. Further he is also the Head of the doctoral school on wireless communication with some 100 Ph.D. students enrolled. His research has focused on radio communication for mobile terminals especially small Antennas, Diversity systems, Propagation and Biological effects and he has published more than 175 peer-reviewed papers and holds 28 patents. He has also worked as consultant for developments of more than 100 antennas for mobile terminals including the first internal antenna for mobile phones in 1994 with lowest SAR, first internal triple-band antenna in 1998 with low SAR and high TRP and TIS, and lately various multi antenna systems rated as the most efficient on the market. He has worked most of the time with joint university and industry projects and have received more than 12 M\$ in direct research funding. Latest he is the project leader of the SAFE project with a total budget of 8 M\$ investigating tunable front end including tunable antennas for the future multiband mobile phones. He has been one of the pioneers in establishing Over-The-Air (OTA) measurement systems. The measurement technique is now well established for mobile terminals with single antennas and he was chairing the various COST groups (swg2.2 of COST 259, 273, 2100 and now ICT1004) with liaison to 3GPP for over-the air test of MIMO terminals.